

4.3.7 Influence of testing machine stiffness

Figure 4.6 illustrates the interaction between a specimen and a conventional testing machine. The specimen and machine are regarded as springs loaded in parallel. The machine is represented by a linear elastic spring of constant longitudinal stiffness, k_m , and the specimen by a non-linear spring of varying stiffness, k_s .

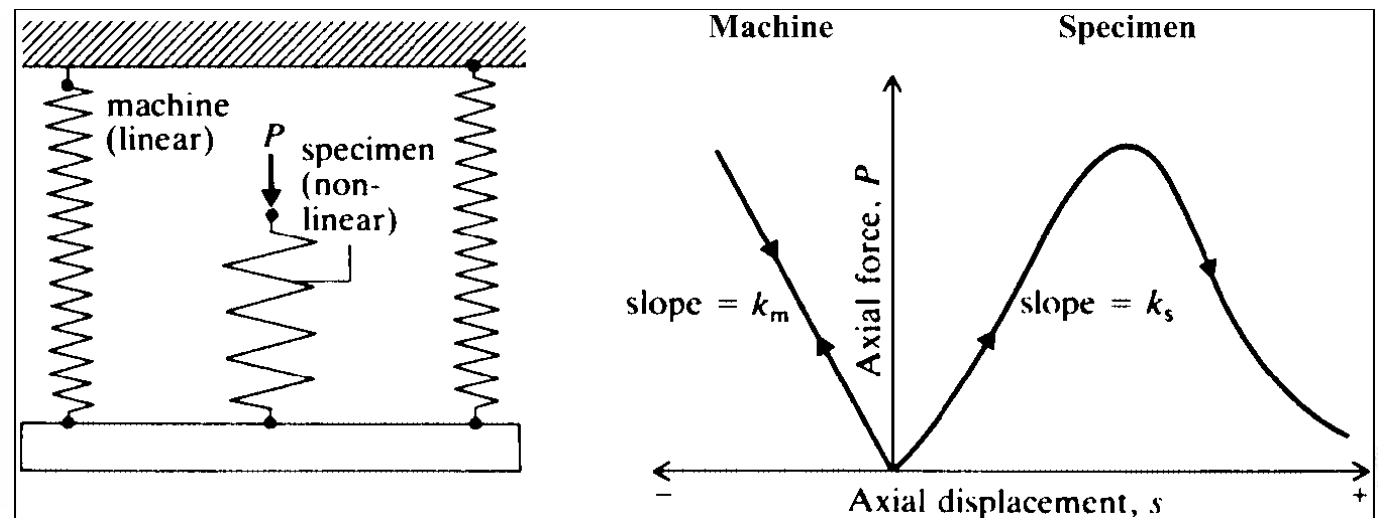
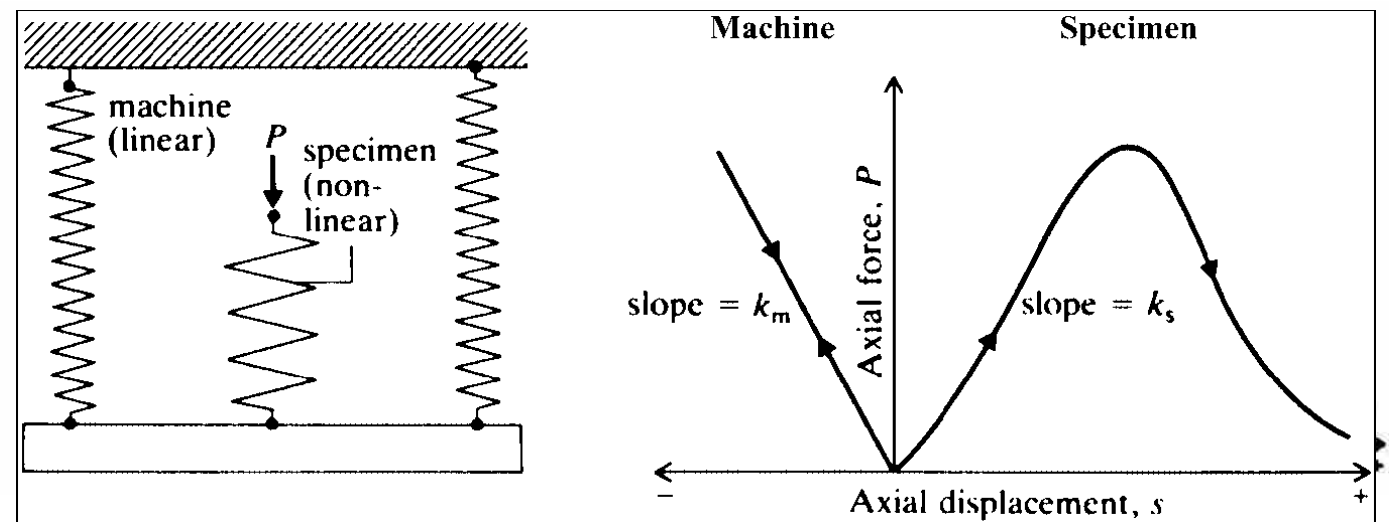


Figure 4.6 Spring analogy illustrating machine-specimen interaction.

4.3.7 Influence of testing machine stiffness

Compressive forces and displacements of the specimen are taken as positive. Thus as the specimen is compressed, the machine spring extends. (This **extension** is analogous to that which occurs in the columns of a testing machine during a compression test.)

Figure 4.6 Spring analogy illustrating machine-specimen interaction.

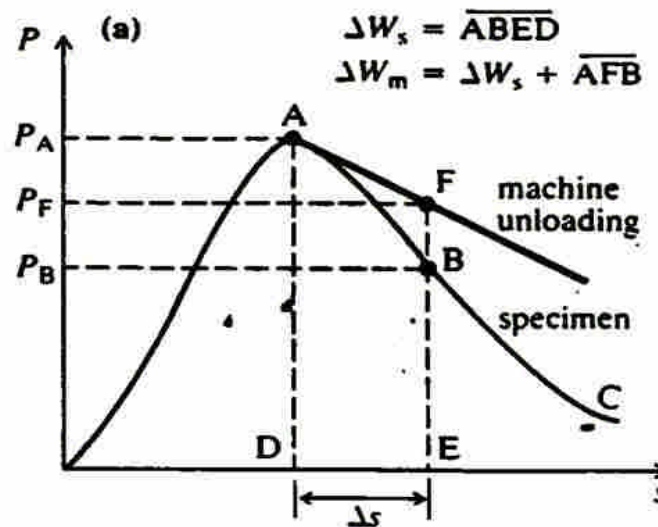


4.3.7 Influence of testing machine stiffness

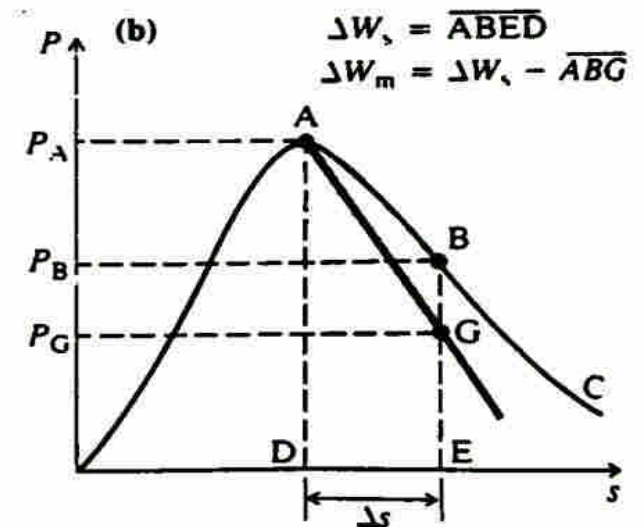
Figure 4.7 shows what will happen if the machine is

(a) soft, and (b) stiff, with respect to the specimen.

Figure 4.7 Post-peak unloading using machines that are (a) soft, and (b) stiff, with respect to the specimen.



(a) Soft Machine

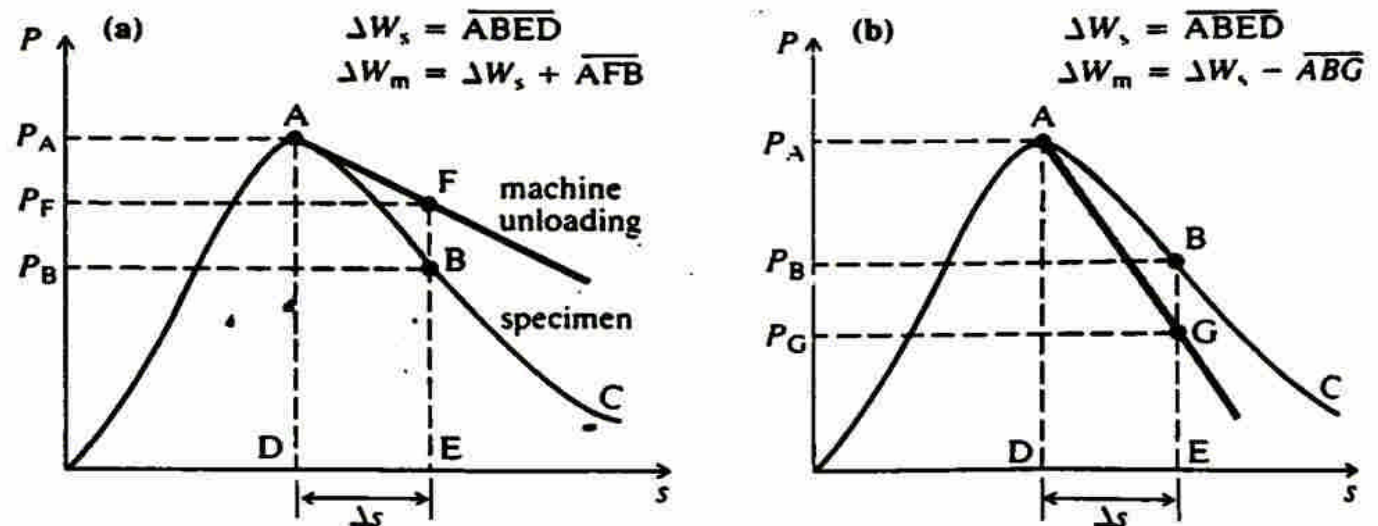


(b) Stiff Machine


4.3.7 Influence of testing machine stiffness

If the machine **is stiff** with respect to the specimen in the post-peak region, the post-peak curve can be followed. $\Delta W_m < \Delta W_s$ and energy in excess of that released by the machine as stored **strain energy** must be **supplied** in order to deform the specimen along ABC.

Figure 4.7 Post-peak unloading using machines that are (a) soft, and (b) stiff, with respect to the specimen.



4.3.7 Influence of testing machine stiffness

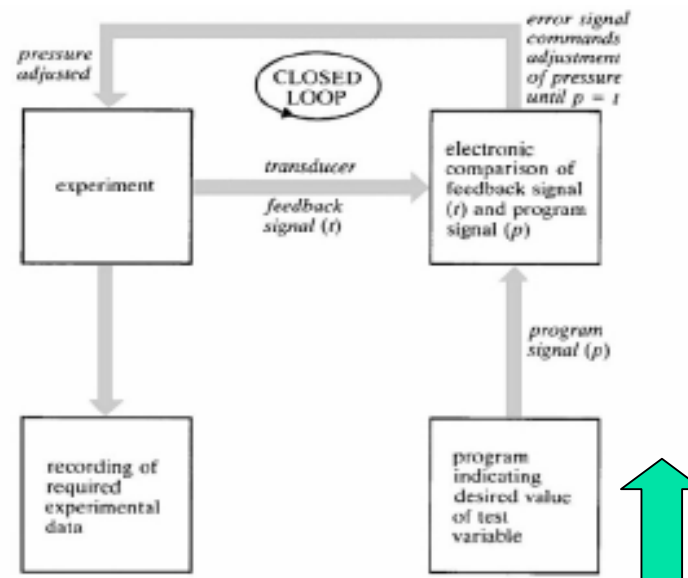


For some very brittle rocks, generally those that are fine grained and homogeneous, portions of the post-peak force-displacement or stress-strain curves can be very steep so that it becomes impossible to 'control' post-peak deformation even in the stiffest of testing machines. In these cases, the post-peak curves and the associated mechanisms of fracture may be studied using a judiciously operated servocontrolled testing machine.

4.3.7 Influence of testing machine stiffness

Closed-loop servocontrol are . An experimental variable (a force, pressure, displacement or strain component) is programmed to vary in a predetermined manner,

Figure 4.8 Principle of closed-loop control (after Hudson *et al.*, 1972b):

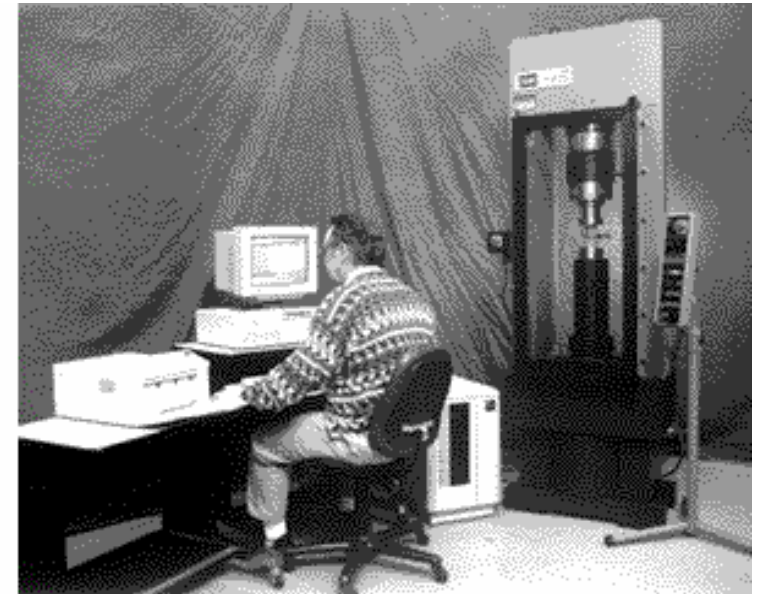


4.3.7 Influence of testing machine stiffness

Uniaxial Rock Mechanics Test Systems

How To Get Power With Precision Control
For Your **Brittle Materials**

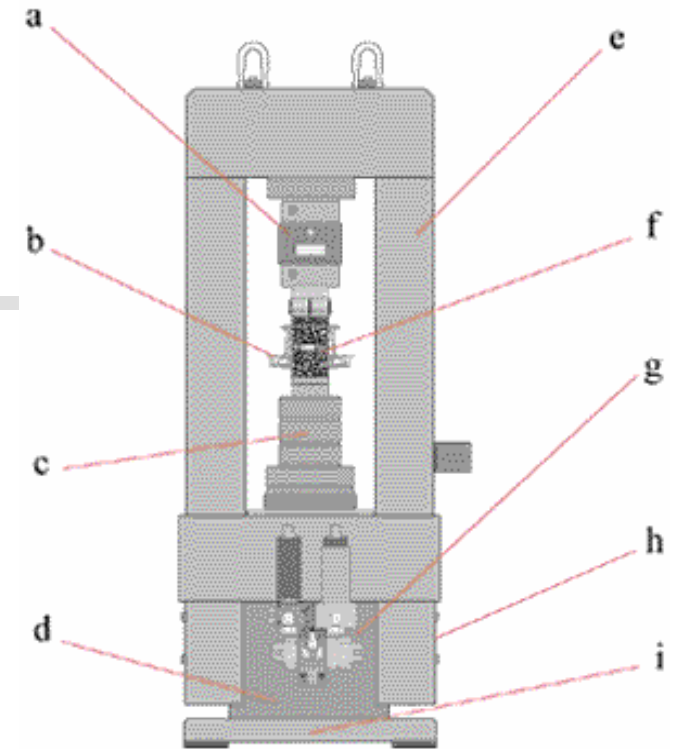
A **Stiff, High Force, MTS load frame** is integrated with a responsive servo-hydraulic performance package, on-the-specimen instrumentation, test fixtures, fully digital controls and application software.



4.3.7 Influence of testing machine stiffness

The result is a precision brittle materials test instrument.

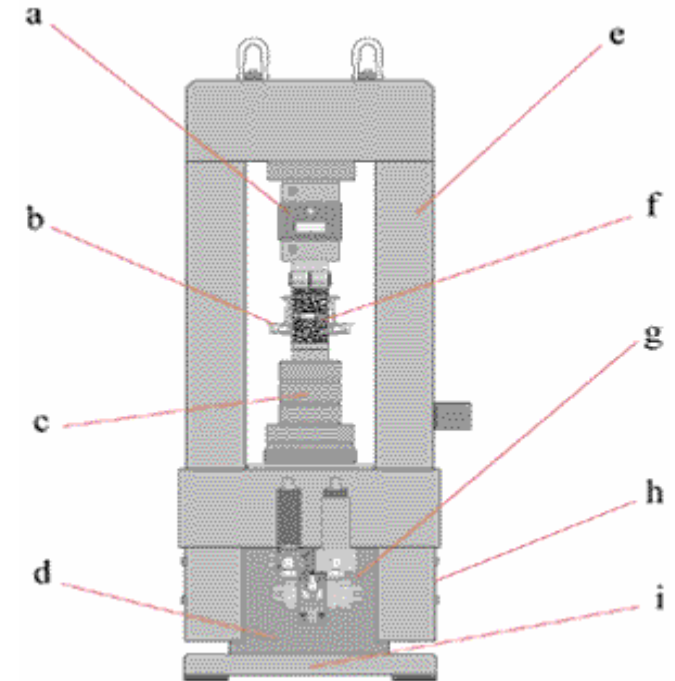
- a. **Strain-gaged load cells** are available for accurate control and measurement of force when testing small or fragile specimens.
- b. **Axial extensometers** attach directly to the specimen to measure and control axial strain over a specified gage length, reducing the effect of unpredictable specimen-end cap friction.



4.3.7 Influence of testing machine stiffness

c. **Spacer plates** permit use of a short stroke actuator, reducing **hydraulic compliance** to further stiffen the load train and improve test control.

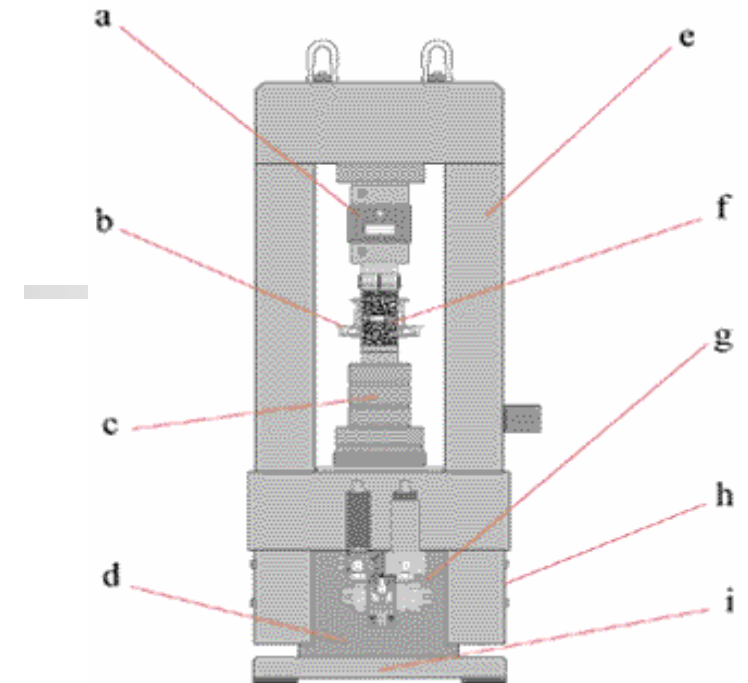
d. **The large diameter actuator bearing** is integrated into the load frame baseplate for high resistance to rod bending, reducing the chance of premature or non-representative specimen failure. You can control both compressive and tensile loads with the double acting high force actuator.



4.3.7 Influence of testing machine stiffness

e. **Solid steel columns** provide an exceptionally stiff load frame that stores a minimum amount of elastic energy giving you better control of brittle specimen failure.

f. **The low-friction chain kit** of MTS **circumferential extensometers** controls and measures overall lateral specimen deformation, not just discrete points.

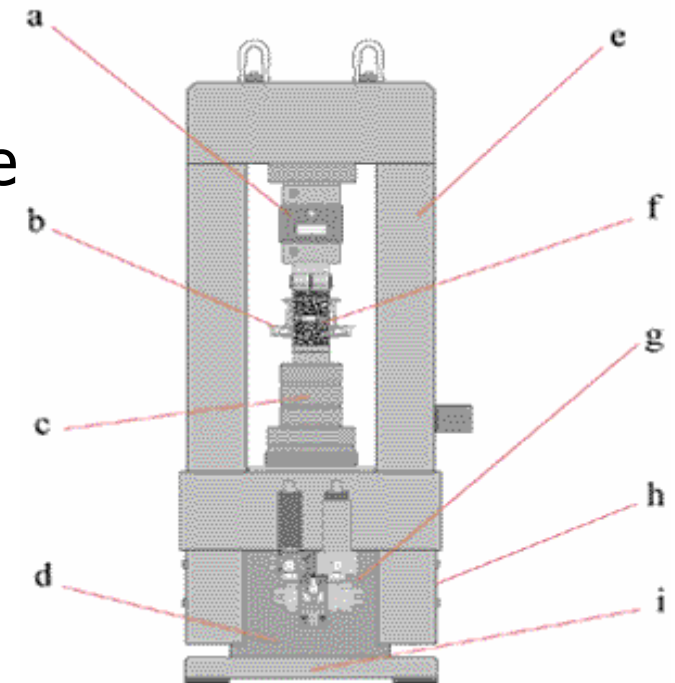


4.3.7 Influence of testing machine stiffness

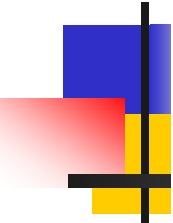
g. Close-coupled, high speed **servo-valves** and **hydraulic accumulators** give you the crisp response you need to control cyclic or post failure tests of brittle specimens.

h. **A differential pressure transducer** provides closed loop control for high force testing of large specimens.

i. Coaxial mounting of the **LVDT** displacement transducer eliminates misalignment to provide reliable stroke control and measurement.

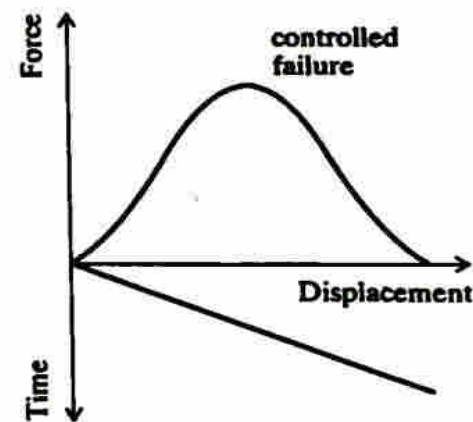
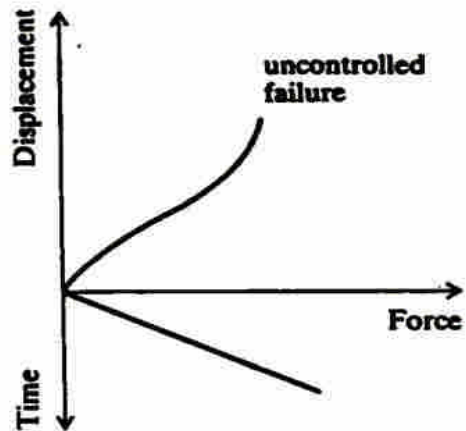


4.3.7 Influence of testing machine stiffness



Modern servocontrolled testing systems are used to conduct a wide variety of tests in rock mechanics laboratories. The key to the successful use of these systems is the choice of the control variable. The basic choice, is between a force (or stress) and a displacement (or strain) component.

4.3.7 Influence of testing machine stiffness



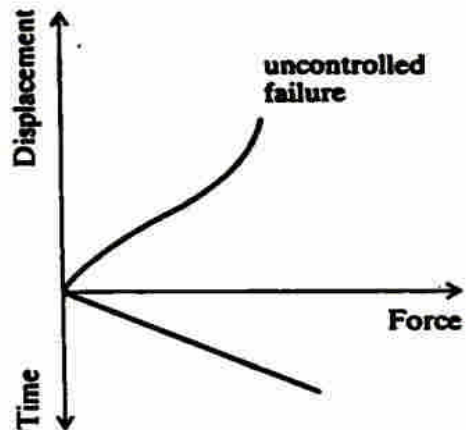
It is **not feasible** to obtain the **complete uniaxial force-displacement curve** for a **strain-softening** specimen by programming the **axial force** to increase monotonically with time.

Read Goodman(1989) p.79~80

3.5 Applications of the **Complete Stress-Strain Curve**

Figure 4.9 Choice between force and displacement as the programmed control variable (after Hudson *et al.*, 1972a).

4.3.7 Influence of testing machine stiffness



The test can be successfully controlled by programming the axial displacement to increase monotonically with time.

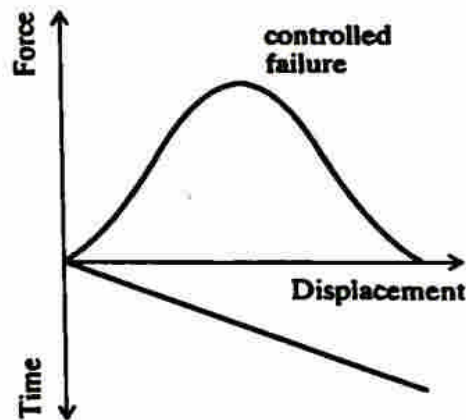
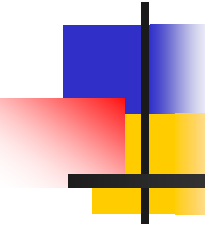


Figure 4.9 Choice between force and displacement as the programmed control variable (after Hudson *et al.*, 1972a).

4.3.7 Influence of testing machine stiffness



The post-peak portions of the force-displacement curves obtained in compression tests on some rocks may be steeper, or not smooth . In these cases, better control can be obtained by using the circumferential displacement rather than the axial displacement as the control variable.

4.3.7 Influence of testing machine stiffness

Figure 4.10 shows the complete axial stress (σ_a)-axial strain (ϵ_r) and circumferential (or radial) strain (ϵ_a)-axial strain curves obtained in such a test on a 50 mm diameter by 100 mm long specimen of an oolitic limestone (鮎狀石灰岩 Portland stone) in which a wrap-around transducer was used to monitor circumferential displacement.

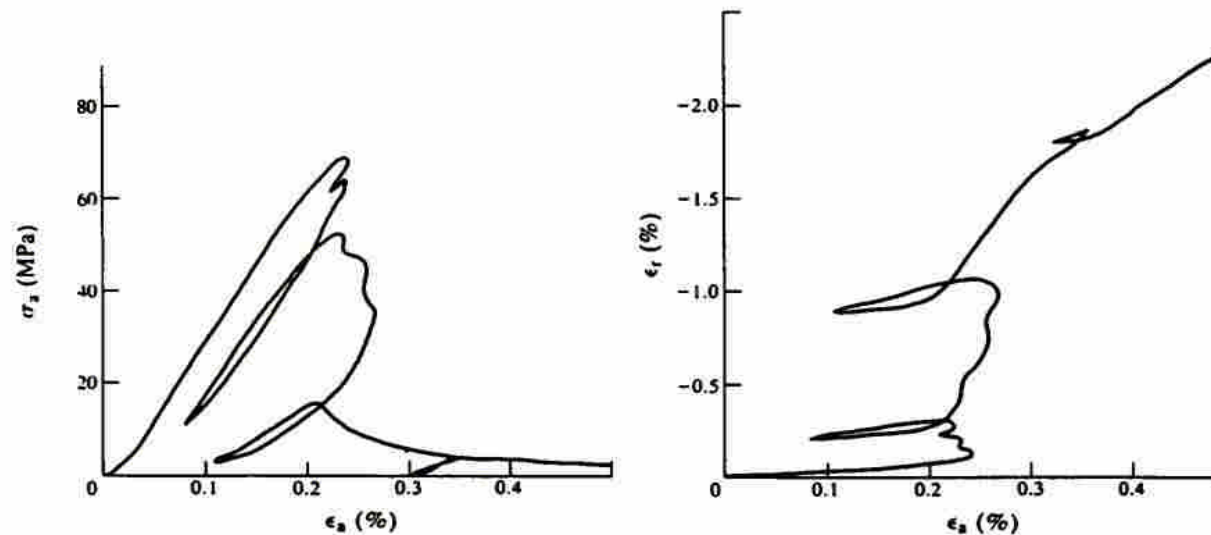
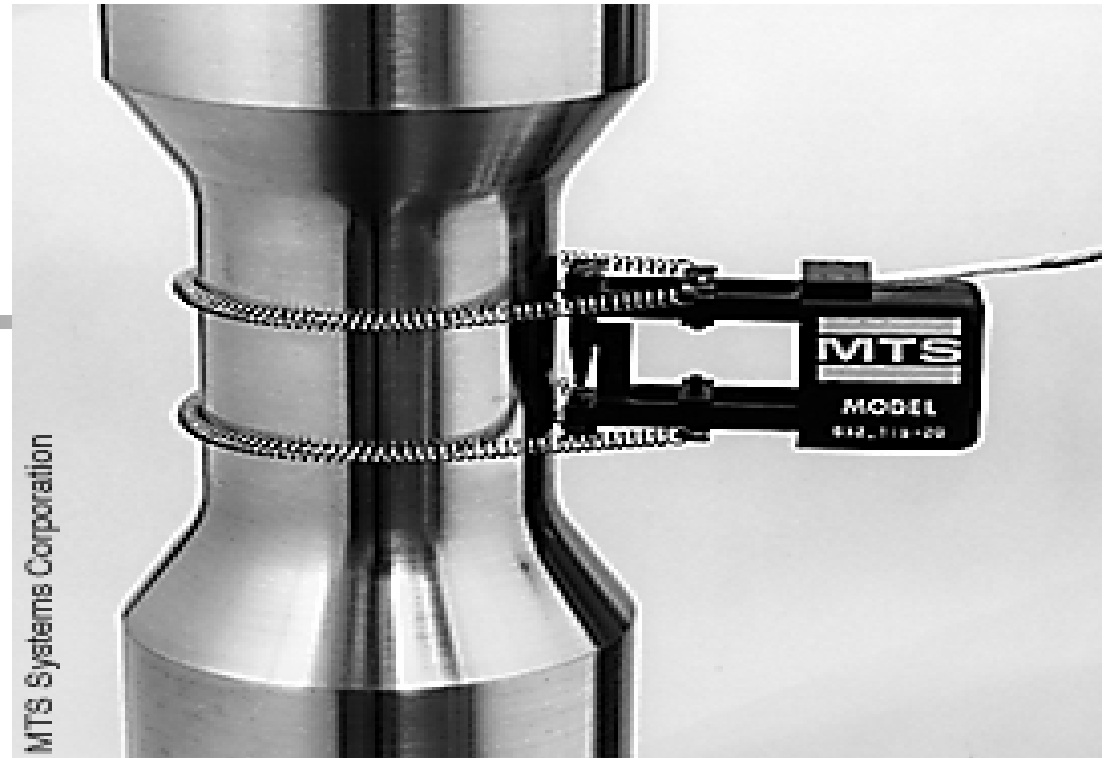


Figure 4.10 Axial stress, σ_a , and radial strain, ϵ_r , vs. axial strain, ϵ_a , curves recorded in a uniaxial compression test on an oolitic limestone (鮎狀石灰岩 Portland stone).

4.3.2 Standard test procedure and interpretation

Large Diameter Specimen Attachment Kit As the diameter of a specimen increases, the normal force holding the **extensometer** in place is reduced. Under such circumstances, this kit provides for a more effective attachment angle, resulting in increased normal force for proper stability. This kit includes two remote spring attachment bracket assemblies that mount on the extensometer arms, and an assortment of 16 tension springs. The large diameter specimen attachment kit expands your range of testing capabilities. Use with models 632.11/12/25 and 634.11/12/25 on specimens larger than 1.25 in. (32 mm) in diameter.



4.3.7 Influence of testing machine stiffness

The complete $\sigma_a - \epsilon_a$ curves obtained by Wawersik and Fairhurst (1970) in a series of controlled uniaxial compression tests on a range of rock types.

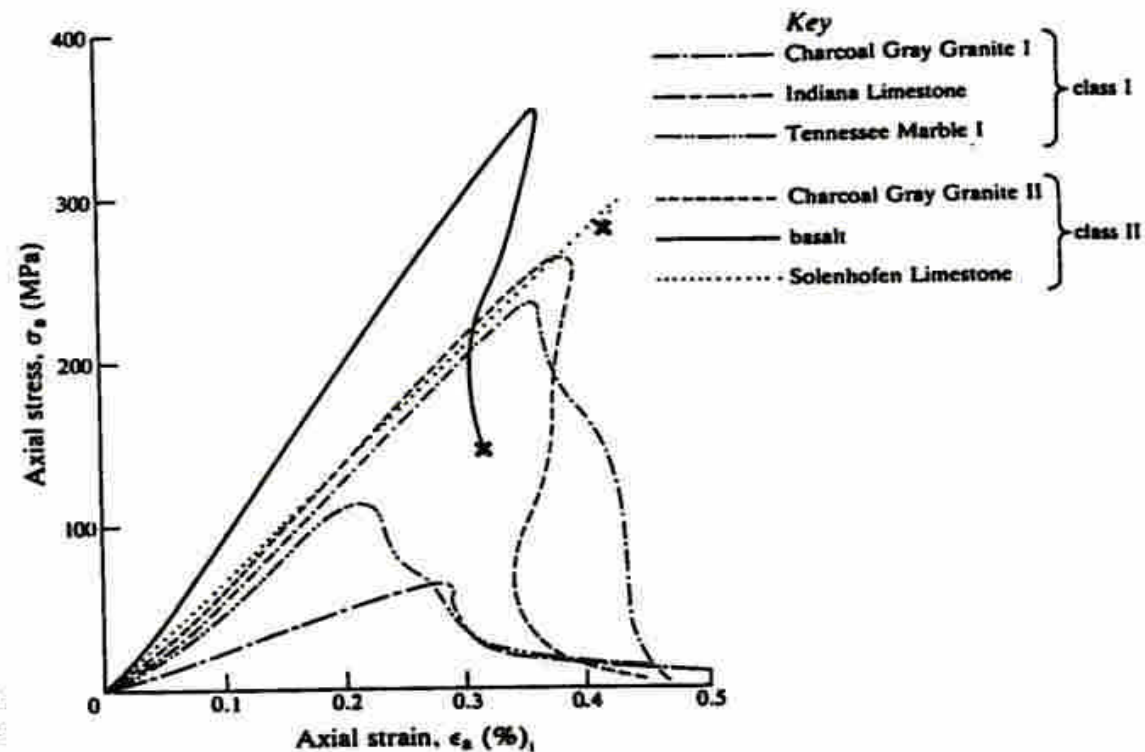


Figure 4.11. Uniaxial stress-strain curves for six rocks (after Wawersik and Fairhurst, 1970).

4.3.7 Influence of testing machine stiffness

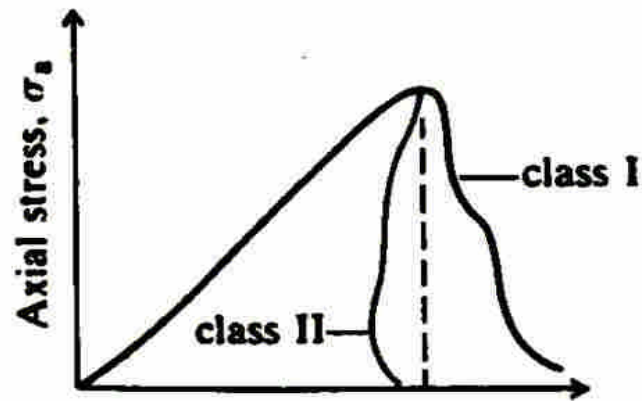


Figure 4.12 Two classes of stress-strain behavior observed in uniaxial compression tests (after Wawersik and Fairhurst, 1970).

The post-peak behaviours of the rocks may be divided into two classes :

Class I behaviour, fracture propagation is stable in the sense that **work must be done** on the specimen for each incremental decrease in load-carrying ability.

Class II behaviour, the fracture process is unstable or self-sustaining; to control fracture, **energy must be extracted** from the material.

4.3.7 Influence of testing machine stiffness

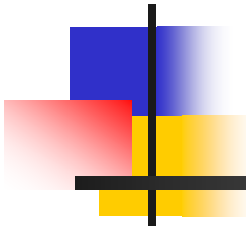
The experiments of Wawersik and Fairhurst indicates that, in uniaxial compression, two different modes of fracture may occur:

(a) Local Tensile Fracture parallel


to the applied stress; (initiald at 50~95% of Peak Strength) Class I

(b) Local and Macroscopic Shear Fracture

(faulting). ; (initiald at Post Peak) Class II




4.3.7 Influence of testing machine stiffness



In very heterogeneous rocks, sub-axial fracturing is often the only fracture mechanism associated with the peaks of the $\sigma_a - \varepsilon_a$ curves for both class I and class II behaviour. In such rocks, shear fractures develop at the boundaries and then in the interiors of specimens, well beyond the peak. This observation is at variance with the traditional view that through-going shear fracture occurs at the peak. Generally, these shear fractures, observed in 'uncontrolled' tests, are associated with sudden unloading in a soft testing machine.

4.3.7 Influence of testing machine stiffness



In homogeneous, fine-grained rocks such as the Solenhofen Limestone (Figure 4.11, class II), the peak compressive strength may be governed by **Localised faulting**.

Because of the internal structural and mechanical homogeneity of these rocks, there is an **absence of the local stress concentrations** that may produce **pre-peak cracking** throughout coarser-grained crystalline aggregates.

4.3.7 Influence of testing machine stiffness

In these homogeneous, fine-grained rocks (can be considered as class II), fracture initiation and propagation can occur almost simultaneously.

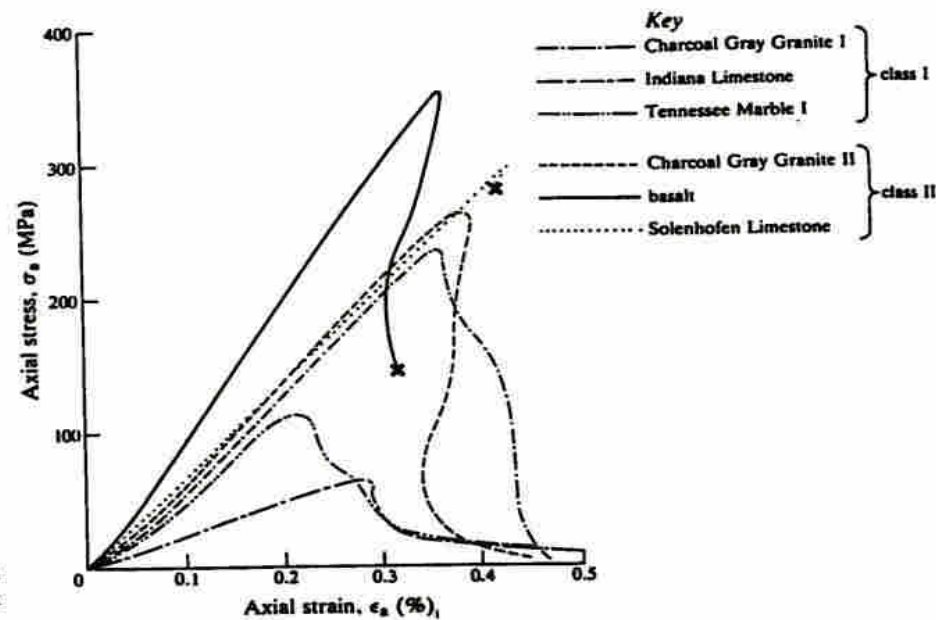



Figure 4.11. Uniaxial stress-strain curves for six rocks (after Wawersik and Fairhurst, 1970).

4.3.7 Influence of testing machine stiffness



It is important to recognise that the post-peak portion of the curve does not reflect a true material property.

4.3.8 Influence of loading and unloading cycles

Figure 4.13 shows the axial force-axial displacement curve obtained by [Wawersik and Fairhurst \(1970\)](#) for a 51 mm diameter by 102 mm long specimen of Tennessee Marble which was unloaded and then reloaded from a number of points in the post-peak range.

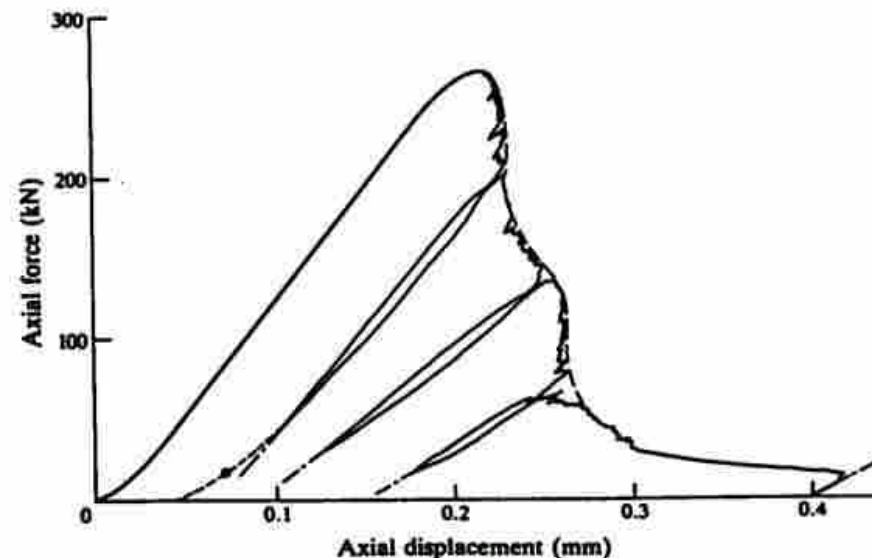


Figure 4.13 Axial force-axial displacement curve obtained for Tennessee Marble with post-peak unloading and reloading (after Wawersik and Fairhurst, 1970).

4.3.8 Influence of loading and unloading cycles

Several points should be noted about the behaviour observed.

- (a) On reloading, the curve eventually joins that for a specimen in which the axial displacement increases monotonically with time.

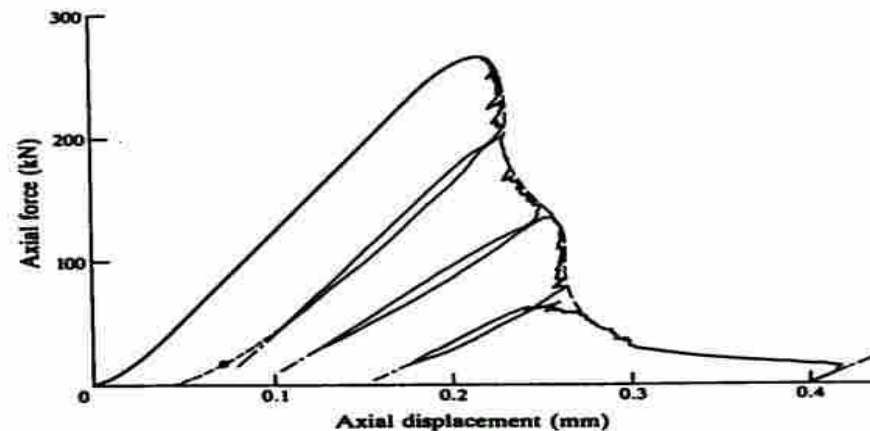


Figure 4.13 Axial force-axial displacement curve obtained for Tennessee Marble with post-peak unloading and reloading (after Wawersik and Fairhurst, 1970).

4.3.8 Influence of loading and unloading cycles

Several points should be noted about the behaviour observed.

- (b) As displacement continues in the post-peak region, the proportion of the total displacement that is irrecoverable increases.

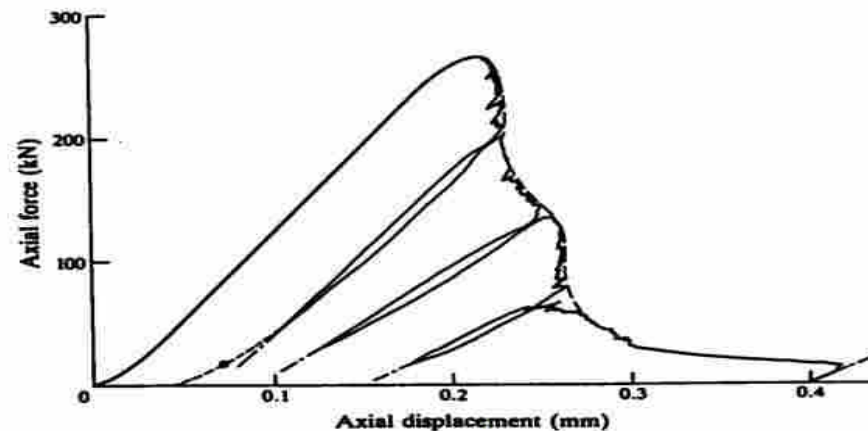


Figure 4.13 Axial force-axial displacement curve obtained for Tennessee Marble with post-peak unloading and reloading (after Wawersik and Fairhurst, 1970).

4.3.8 Influence of loading and unloading cycles

(c) The unloading-loading loop shows some hysteresis .

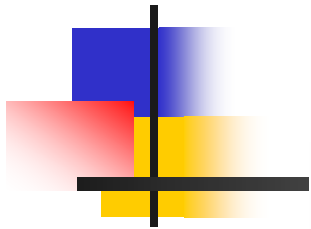
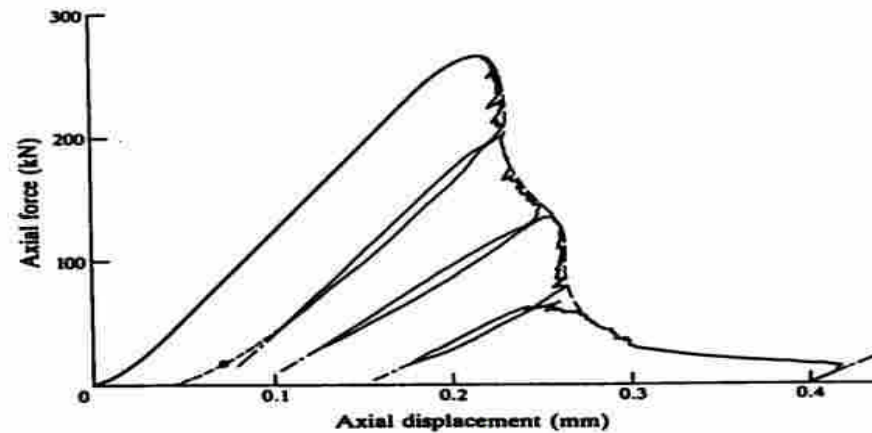


Figure 4.13 Axial force–axial displacement curve obtained for Tennessee Marble with post-peak unloading and reloading (after Wawersik and Fairhurst, 1970).



4.3.8 Influence of loading and unloading cycles

Several points should be noted about the behaviour observed.

- (d) The apparent modulus of the rock which can be calculated from the slope of the reloading curve, decreases with post-peak deformation and progressive fragmentation of the specimen.

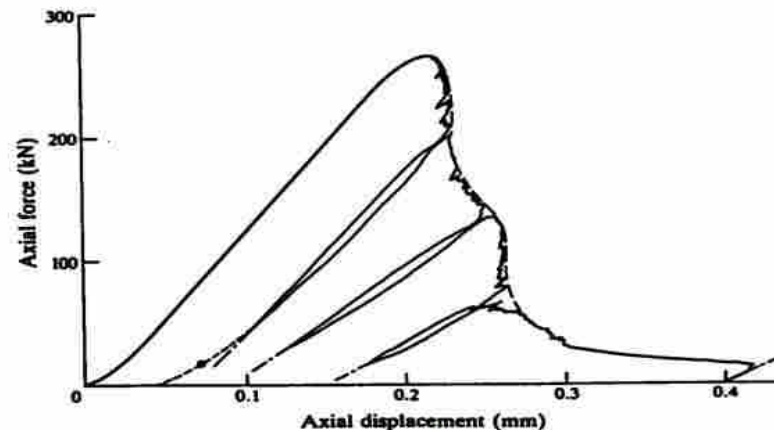
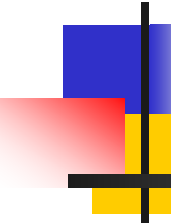


Figure 4.13 Axial force-axial displacement curve obtained for Tennessee Marble with post-peak unloading and reloading (after Wawersik and Fairhurst, 1970).

4.3.8 Influence of loading and unloading cycles



If rock specimens are subjected to loading and unloading cycles in the pre-peak range, some **permanent deformation** and **hysteresis** are generally observed. This is often associated with 'bedding-down' effects, and for this reason, the ISRM Commission (1979) recommends that it is sometimes advisable for **a few cycles of loading and unloading** to be performed.

4.3.9 The point load test

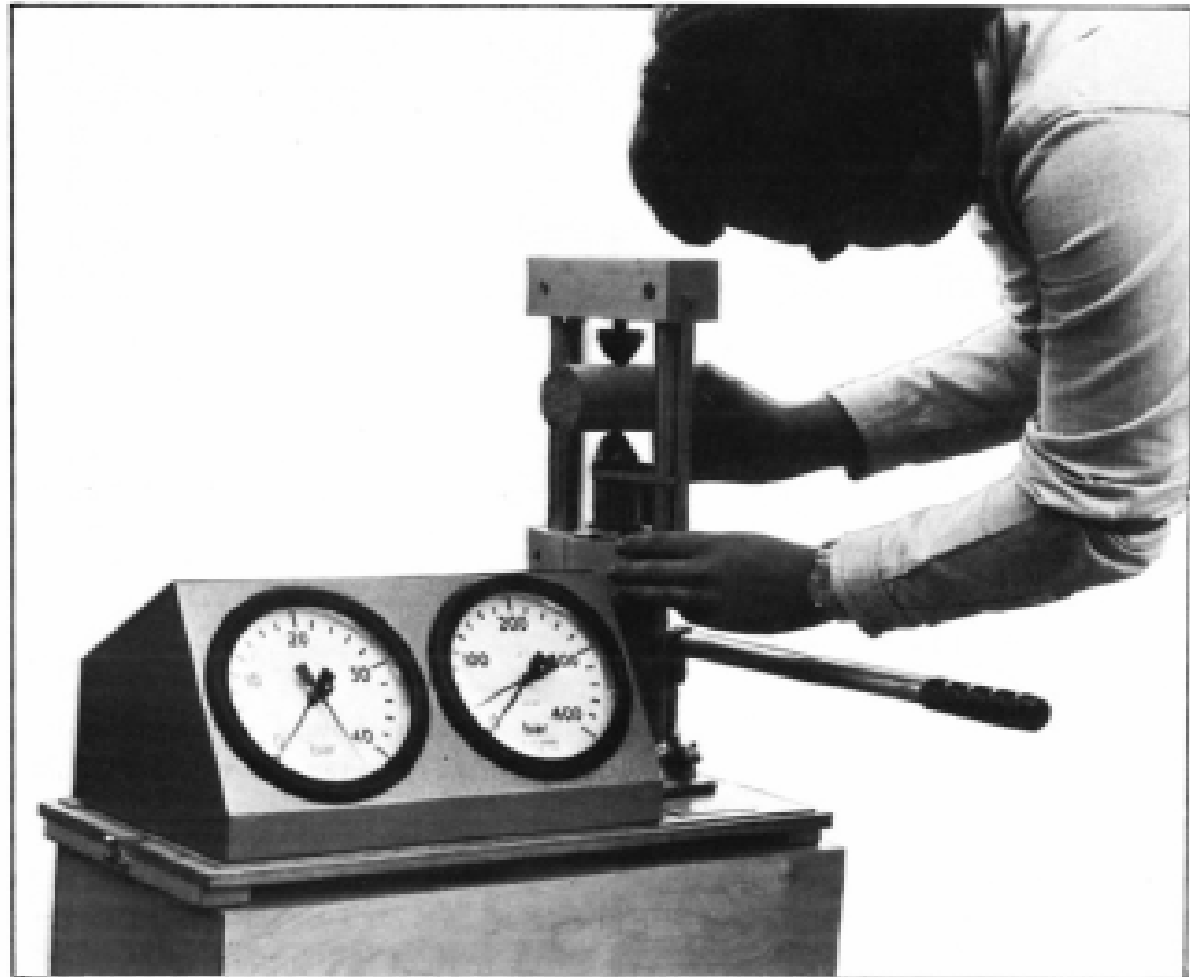


Figure 4.14 Point load test apparatus (photograph by ELE International Ltd).

4.3.9 The point load test

A point load index (Uncorrected)


$$I_s = \frac{P}{D_e^2} \quad (4.5)$$

D_e : equivalent diameter $= 4A / \pi$

$$I_{s(50)} \cong I_s (D_e / 50)^{0.45} \quad (4.6)$$

The uniaxial compressive strength

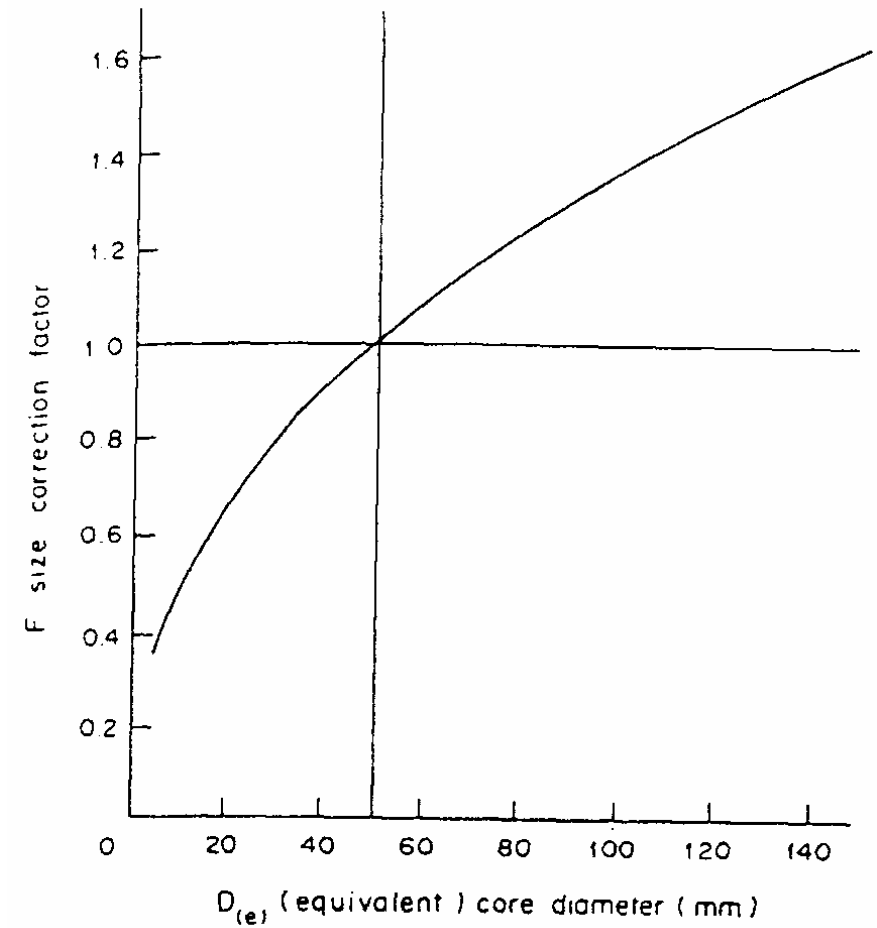
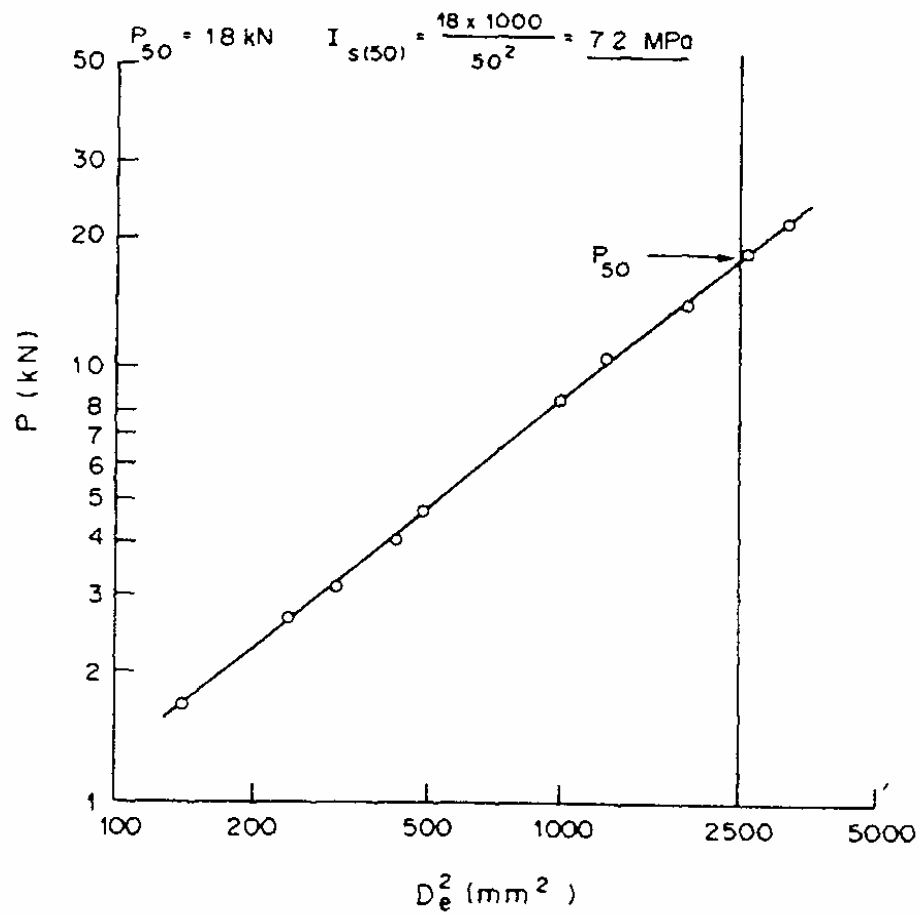
$$\sigma_c \cong (22 \sim 24) I_{s(50)} \quad (4.7)$$



The Point Load Test

- I_s : *The uncorrected point load strength*
 - P/D_e^2
 - P: Load
 - D_e : Equivalent core diameter
 - $D_e^2 = D^2$ for diametral test
 - = $4A/\pi$ for axial, block, and lump tests
 - $A = WD$ = minimum cross sectional area of a plane through the contact point.

The Point Load Test - Size correction





The Point Load Test


- $I_{S(50)} = F \times I_S$
 - $F = (D_e/50)^{0.45}$

4.3.9 The point load test

The test is one in which fracture is caused by induced tension, and it is essential that a consistent mode of failure be produced if the results obtained from different specimens are to be comparable.




4.3.9 The point load test



Very soft rocks, and highly anisotropic rocks or rocks containing marked planes of weakness such as bedding planes, are likely to give spurious results. A high degree of scatter is a general feature of point load test results and large numbers of individual determinations (often in excess of 100) are required in order to obtain reliable indices.

4.3.9 The point load test

For anisotropic rocks,



Strength Anisotropy Index, $I_{a(50)}$, defined as the ratio of mean $I_{s(50)}$ values measured perpendicular and parallel to the planes of weakness.



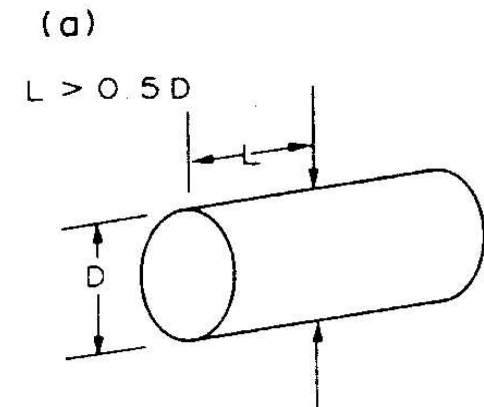
The Point Load Test

- Suggested method for determining point load strength
 - *Int, J. Rock Mech. Min. Sci. & Geomech. Abstr. Vol. 22, No. 2, pp. 51-60,1985*
- 1. A set of rock specimens of similar strength
- 2. Contain sufficient specimens conforming with the size and shape requirements
- 3. Tested at either fully water-saturated or natural water content

The Point Load Test

- *The diametral test*

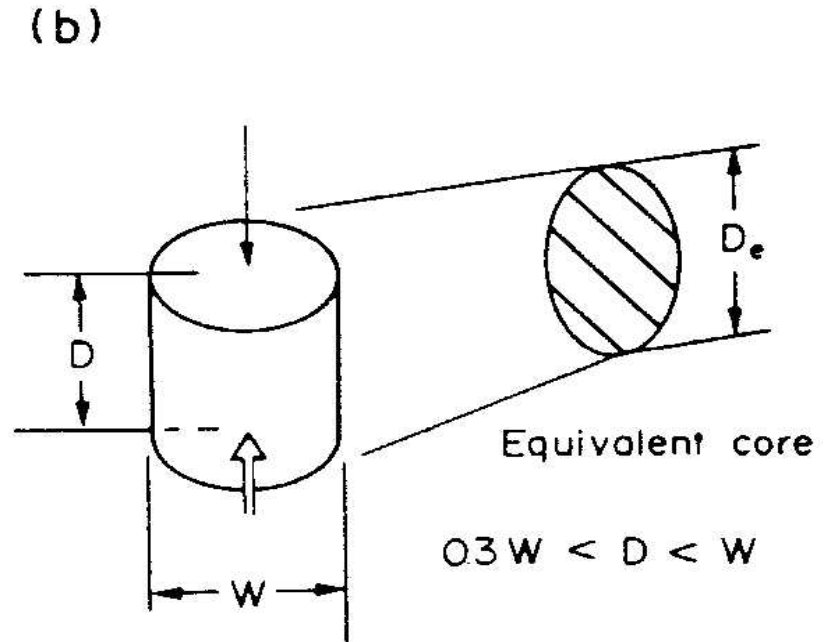
- L/D greater than 1.0
- At least 10 tests for sample
- The points of contact should be nearly at a diameter
- Distance between point of contact and each free end (L) should be at least 0.5 times the diameter



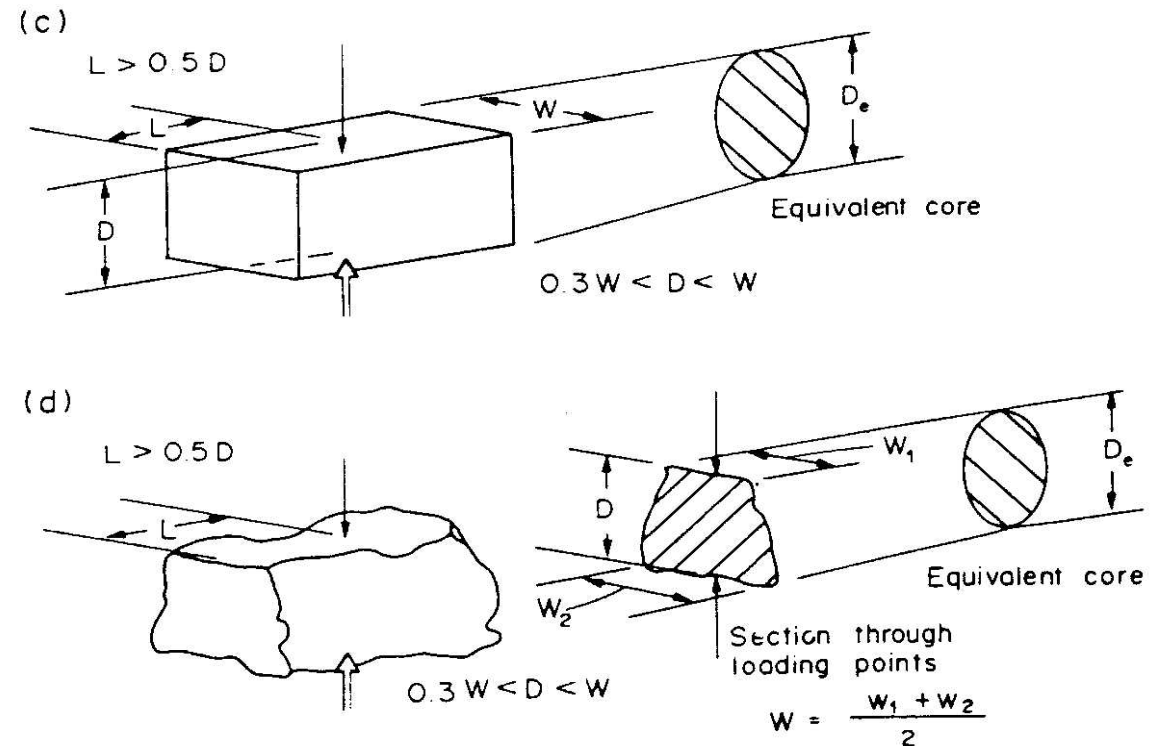
The Point Load Test

■ *The axial test*

- D/W of 0.3~1.0
- At least 10 test for sample
- Two contact points should be along a line that perpendicular to the end surface of a core
- Load steadily increased such that failure occurs within 10-60 sec.



The Point Load Test



- *The block and irregular lump tests*
 - D/W at $0.3 \sim 1.0$
 - Contact at a **smallest dimension** away from corners or edges
 - Load steadily increased such that failure occurs within **10-60 sec.**



The Point Load Test

- *Anisotropic Rock*
 - At directions of **parallel** and **normal** to the planes of anisotropy
 - Core with weakness planes and perform diametral test at some interval that would yield some sufficient specimens for axial test
 - Angle of the core axis and weakness plane should not excess 30 degrees
 - Ensure the load is applied along the single weakness plane to obtain the least I_s , and perpendicular to the weakness plane to obtain the largest I_s



Direct Tensile Strength Test

The method, in principle, is similar to that employed in the testing of metals. There are **difficulties in gripping the specimens** and **applying a load parallel to the axis of the specimen**. It is important that the specimen is mounted in tension **grips without damaging the surface of the specimen**.

Direct Tensile Strength Test

If the load cannot be applied **parallel to the axis of the specimen**, there will be a tendency to cause bending, producing **abnormal stress concentrations**.

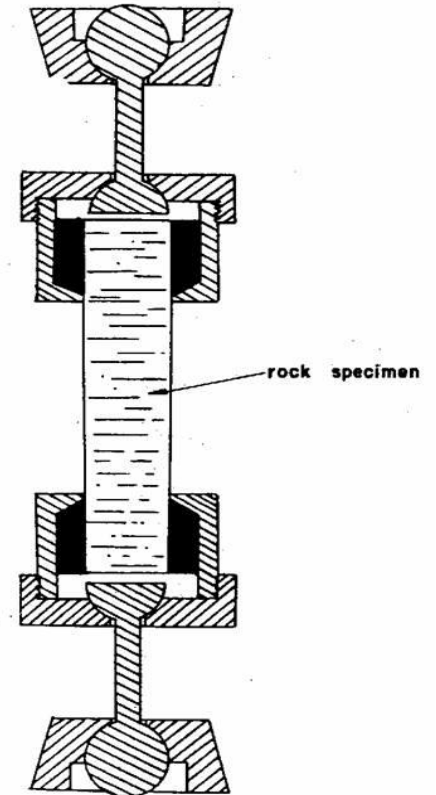


Fig. 3-1. Grips for tensile strength test (after OBERT, WINDES and DUVALL, 1946).

Direct tensile strength Test (Tensile Strength of Rock)

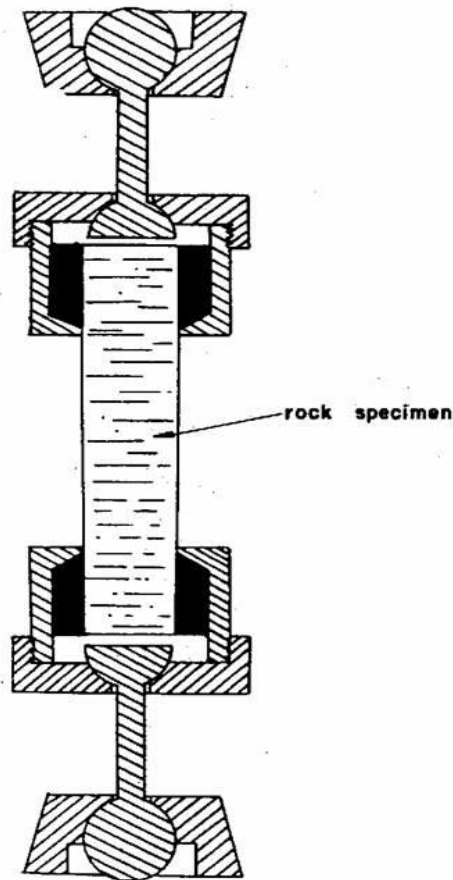


Fig. 3-1. Grips for tensile strength test
(after OBERT, WINDES and DUVAL, 1946).

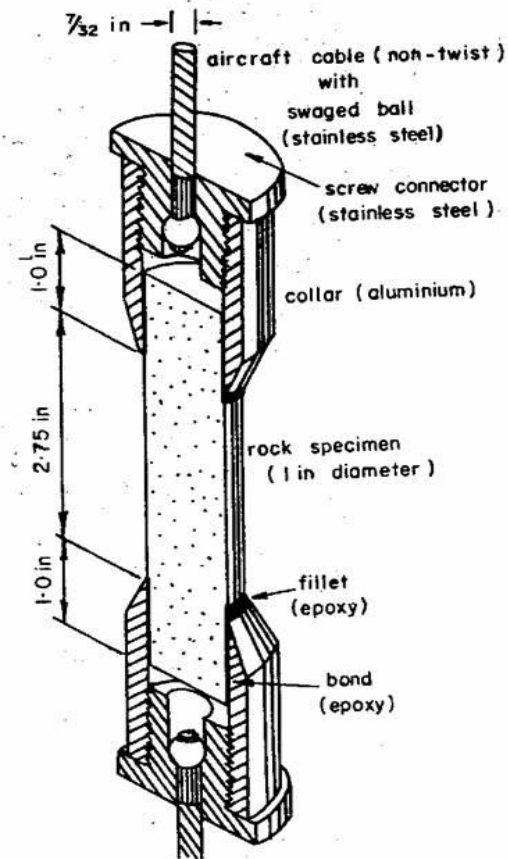
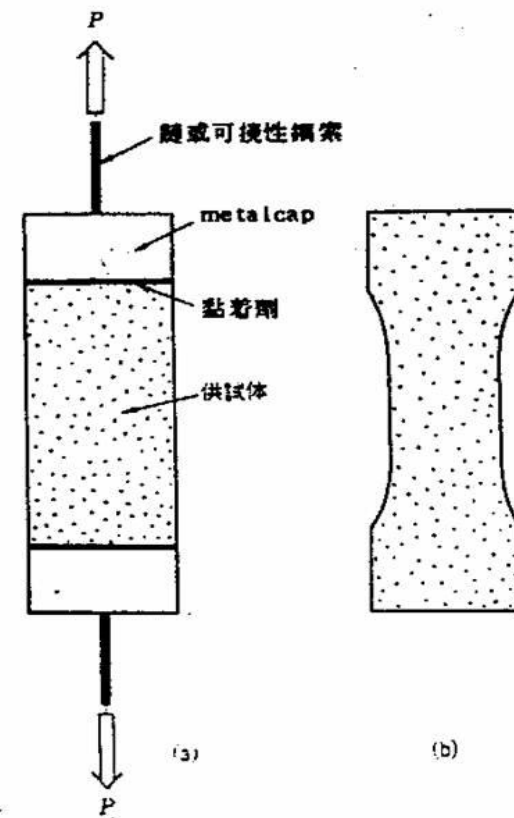
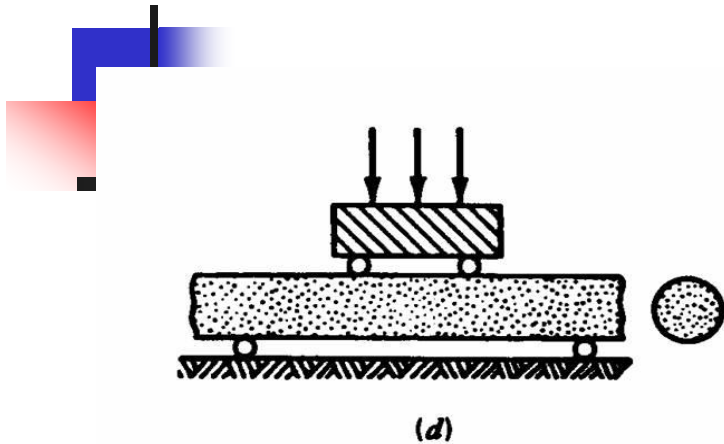


Fig. 3-4. Chamfered collar method for uniaxial tensile test
(after HAWKES and MELLOR, 1970).



圖一 9•10 直接拉力試驗

Four-point Bending Test

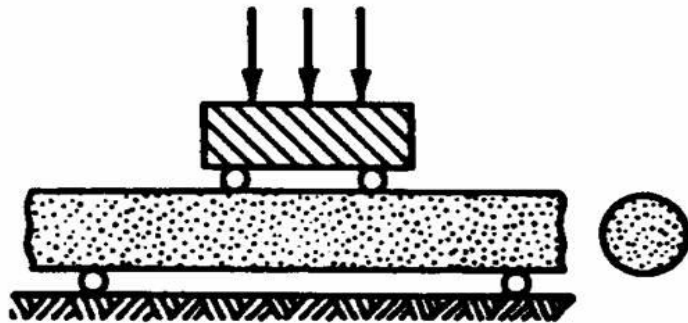


For **four-point bending** of cylindrical rock specimens, with **loads applied at $L/3$** from each end and reactions at the ends, the **modulus of rupture (MR)** is:

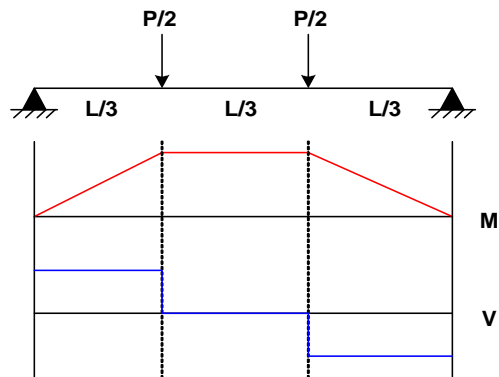
$$T_{MR} = \frac{16 P_{\max} L}{3\pi d^3}$$

Where P_{\max} is the maximum load, L is the length between load reactions on the lower surface, and d is the diameter of the core.

Four-point Bending Test



(d)



圓柱的 I 值

$$I = \frac{\pi r^4}{4} \quad \sigma = \frac{My}{I}$$

$$\begin{aligned} T_{MR} = \sigma &= \frac{My}{I} = \frac{\frac{PL}{6} \cdot r}{\frac{\pi r^4}{4}} = \frac{2PL}{3\pi r^3} \\ &= \frac{2PL}{3\pi d^3} \cdot 8 = \frac{16PL}{3\pi d^3} \end{aligned}$$